Tribocorrosion behaviours of cold-sprayed diamond–Cu composite coatings in artificial sea water

Zhe Wang, Xiuyong Chen, Yongfeng Gong, Xiaoyan He, Yingkang Wei & Hua Li

📅 Published online: 18 Sep 2017.

✎ Submit your article to this journal ↗

📊 Article views: 9

🔍 View related articles ↗

▣ View Crossmark data ↗

Tribocorrosion behaviours of cold-sprayed diamond–Cu composite coatings in artificial sea water

Zhe Wang[a,b], Xiuyong Chen [a], Yongfeng Gong[a], Xiaoyan He[a,b], Yingkang Wei[c] and Hua Li [a]

[a]Key Laboratory of Marine Materials and Related Technologies, Zhejiang Key Laboratory of Marine Materials and Protective Technologies, Ningbo Institute of Materials Technology and Engineering, Chinese Academy of Sciences, Ningbo, China; [b]University of Chinese Academy of Science, Beijing, China; [c]State Key Laboratory for Mechanical Behavior of Materials, School of Materials Science and Engineering, Xi'an Jiaotong University, Xi'an, China

ABSTRACT
Frictional components in the marine environment always face a synergistic effect of wear and corrosion. Diamond-based composite coatings are known for their excellent wear performances, but few studies were conducted relating to their marine applications. Herein, diamond–copper composite coatings were successfully deposited on stainless steel 316L plates by the cold spraying, employing diamond powder coated with thin copper (Cu) layer. The diamond–Cu composite coatings with a diamond content of 31.79% were successfully fabricated. The coatings showed significantly enhanced wear resistance tested in artificial sea water with the reduced friction coefficient from 0.32 for the Cu coating to 0.10 for the diamond–Cu coating. Further electrochemical testing showed promoted anti-corrosion performances of the diamond-containing coatings. The newly constructed diamond–Cu coatings show encouraging promises as anti-tribocorrosion layers for marine structures.

Introduction

The exploration of marine resources calls for a great need for marine equipment, while marine frictional components, such as sea water pumps, open hydraulic drive system, and propeller, usually encounter the problems caused by corrosion, wear, biofouling, and even their synergistic impact [1]. To address these problems, one of the most effective approaches is to employ advanced coatings to meet all the requirements [2]. Diamond and diamond-like carbon films have been widely used to improve the wear resistance of engineering materials due to their favourable properties, such as high hardness, chemical inertness, and low friction coefficient [3,4]. However, most of the above coatings were deposited using physical or chemical vapour deposition techniques which call for a high vacuum environment. In addition, large-scale fabrication of diamond-based coatings yet keeps challenging. Therefore, searching appropriate construction techniques is one of the current research goals for the fabrication of diamond-based coatings.

Thermal spray techniques offer advantages such as user-friendliness and cost-efficiency in mass production of coatings for various applications. To date, research progresses have been made in thermal spray fabrication of diamond-based composite coatings [5–7]. However, traditional thermal spray techniques usually fail to achieve high density and high fraction of diamond particles in the coatings, and the processing usually causes oxidation and graphitisation of diamond, leading to poor cohesion between diamond and matrix [5]. Cold spraying (CS) is a relatively new approach and has unique advantages in fabricating thermal sensitive materials coatings for a variety of applications [8–10]. To deposit diamond coatings, a soft phase is always needed to facilitate the deposition process. For example, a dense diamond/NiCrAl composite coating was developed by the CS diamond–NiCrAl composite powder as prepared by mechanical alloying processing [11]. Attempts were also made recently in fabricating diamond-based composite coatings using Ni-coated diamond powder blended with bronze as the starting feedstock [12]. The protective Ni layer is believed to prevent fracture and to ensure similar flight behaviour between diamond and bronze, in turn, giving rise to high deposition efficiency of the diamond particles. Yet, there are, so far, few reports available, elucidating the tribocorrosion behaviours of cold-sprayed diamond-based coatings for marine applications.

This study aims to investigate fabrication by the cold spray of diamond-based composite coatings and their tribocorrosion behaviours in the marine environment. The results shed light on coating fabrication and marine applications of the diamond-containing composites.

CONTACT Xiuyong Chen ✉ chenxiuyong@nimte.ac.cn ✎ Key Laboratory of Marine Materials and Related Technologies, Zhejiang Key Laboratory of Marine Materials and Protective Technologies, Ningbo Institute of Materials Technology and Engineering, Chinese Academy of Sciences, Ningbo, China

Experimental procedures

Commercially available diamond powder (Sino-Crystal Micro-diamond Co. Ltd., China) was used as the starting feedstock. Diamond–Cu composite powder was prepared by an electroless copper plating method. To comparatively investigate the performances of the coatings, both diamond–Cu composite coatings and pure Cu coatings were fabricated. Spherical Cu powder of ~30–50 μm (Tianjiu Changsha Co. Ltd., China) was used to prepare the Cu coatings. A home-installed cold spray system was employed to deposit the coatings. Stainless steel 316L plates (316L, 20 × 30 × 2 mm) were used as substrates. Nitrogen was used as the driving gas with a pressure of 3 MPa and a temperature of 400°C in the prechamber. Nitrogen was also used as the powder carrier gas and the spray distance was 20 mm.

Microstructure of the powder and the coatings was characterised by a field emission scanning electron microscope (FESEM, Quanta FEG 250, U.S.A.). Element analyses were carried out by energy-dispersive X-ray spectra (EDS) equipped with the FESEM. Phases of the powder and the coatings were detected by X-ray diffraction (XRD, D8 Advance, Bruker AXS, Germany) at a scan rate of $0.02^o \ s^{-1}$ using Cu Kα radiation operated at 35 mA and 40 kV.

The corrosive wear behaviours of the coatings were evaluated by sliding wear testing and *in situ* electrochemical measurements in artificial sea water (ASW) prepared according to ASTM D1141–98. Sliding wear testing was performed on a tribometer (Rtec, MFT-3000, U.S.A.) with the ball-on-disc reciprocating mode using the Si_3N_4 balls of 6 mm in diameter as the counterpart. A constant load of 10 N, oscillating stroke of 5 mm, sliding speed of $0.02 \ m \ s^{-1}$, and sliding distance of 72 m were chosen for the testing. The friction coefficient-time plots were recorded automatically and each measurement was performed three times. Based on the wear track depth profiles detected by a surface profiler (Alpha-Step IQ, KLA Tencor, U.S.A.), wear losses of the coatings can be obtained after the sliding testing. Electrochemical characterisation was done with an external potentiostat (Modulab 2100A, Solartron Analytical U.K.) in ASW. A standard saturated calomel electrode was used as the reference electrode and platinum was used as the counter electrode. To examine the tribocorrosion behaviours of the samples, a series of experiments were conducted: (1) corrosive wear testing was carried out in open circuit potential (OCP) condition and the evolution of OCP was recorded; (2) potentiodynamic testing involved measurement of polarisation curves during sliding and corrosion only, and it was initiated after a stable OCP. The electrode potential was raised from −0.5 to 0.5 V at a scanning rate of 0.5 mV s⁻¹.

Results and discussion

Morphologies of the diamond powder and the Cu-coated diamond powder are shown in Figure 1(a,b), respectively. The Cu-coated diamond particles have the size of ~21–58 μm which is suitable for CS. Compared with the starting diamond powder, it is clear that diamond particles are coated with a thin Cu layer (Figure 1(b)). The Cu layer with the thickness of ~1–2 μm can be clearly seen (Figure 1(c)). Further EDS characterisation confirms the existence of the Cu layer (Figure 1(d)). To examine the weight per cent of diamond in the coated particles, the coated particles were etched by ammonium persulfate solution to remove the Cu clad completely. By weighing the powder before and after etching, a diamond fraction of ~43% was revealed.

The topographical and cross-sectional morphologies of the composite coatings were characterised by the SEM (Figure 2) and a schematic illustration of the coating formation mechanism is also proposed (Figure 3). The as-sprayed composite coatings with the thickness of ~70 μm were successfully fabricated. The dark regions in the coating are assigned to diamond particles. It can be observed that the copper part is pretty dense, which is distinct in the cold-sprayed pure copper coating [13]. Diamond particles are strongly embedded in the copper matrix, and the contours of diamond particles are well maintained. However, it is noted that large quantities of small-sized diamond particles circled by the black lines are also present in the coatings (Figure 2(b)). It indicates that large diamond particles might have fractured into small pieces during the deposition process. This phenomenon could be explained by unbearable impact stresses encountered by the diamond particles upon their impingement. These pieces still have strong enough kinetic energy to penetrate into the soft phase. Diamond particles would fortunately have chance to embed into the coating in an intact form at the places where the percentage of soft materials is relatively high. It is noteworthy that some of the diamond particles got bounced away from the substrate or pre-coating when they failed to adhere, leaving traces on the top of the coating (Figure 2(c)). The black lines, shown in Figure 2(c), highlight the areas for the bounced diamond particles. To estimate the diamond content in the composite coating, the EDS analysis was performed. The element content histogram, shown in Figure 2(d), suggests a carbon content of 31.79%. This is a pretty high content of diamond compared with those of diamond-containing composite coatings fabricated using mechanically mixed feedstock [5–7,12,14]. The relatively high content of oxygen suggests that the oxidation of copper took place during the CS. But, the oxidation is very limited, since no copper oxides are detected from the XRD analyses of the
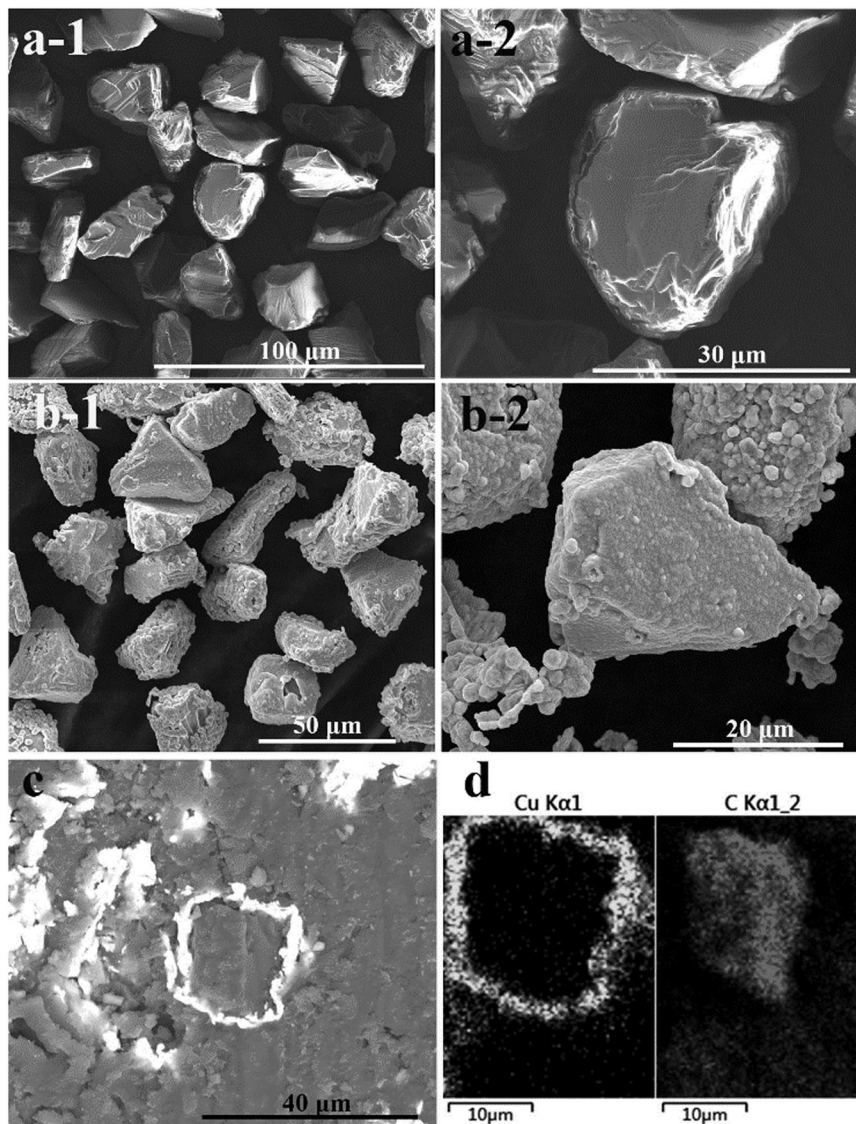
Figure 1. SEM images of the starting diamond powder (a), the Cu-coated diamond powder (-2 is enlarged view of selected area in -1) (b), and the single particle image after polishing (c), (d) EDS result of the image (c) showing complete enwrapping of Cu on diamond particle.

as-sprayed coatings (Figure 4). It is also clear that graphitisation of diamond did not happen during the deposition processing. The results are consistent with a previous report that claimed the cold spray technique to be a potential approach for relieving graphitisation and oxidation of diamond particles [14]. In this case, compared with the XRD peaks for the starting feedstock, the weakened peaks referring to the diamond in the coatings are likely due to the loss of diamond during the coating deposition.

To examine the tribocorrosion behaviours of coatings, OCP measurements are usually performed [15]. It is shown that the OCP drops sharply down to more negative value due to the friction effect at an early stage of the sliding (Figure 5(a)), which is consistent with previous studies [16–18]. The drop in OCP value is believed to be a result of the destruction of passive film formed on the original surface [19]. The contact area is increased by increasing normal load, which
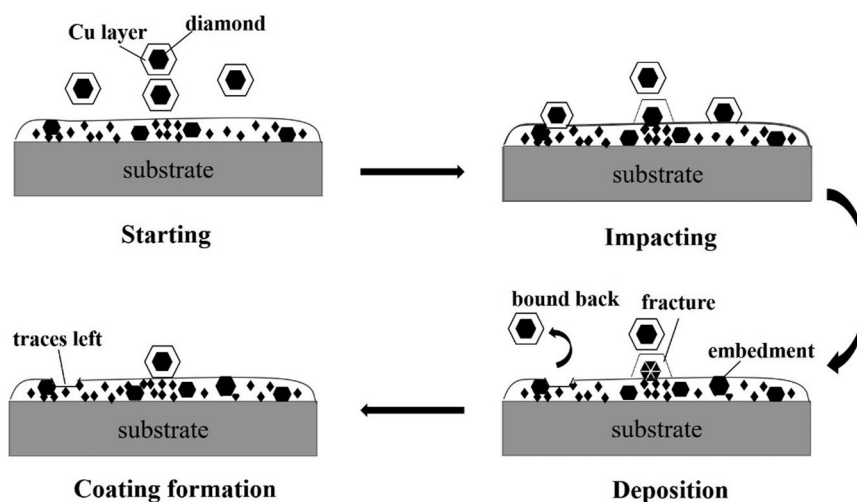
gives rise to enlarged wear track area. As a consequence, an amplified area of active zone would be exposed, in turn, causing drop in OCP. It can be seen that OCP values rise gradually after the sharp dropping at the beginning of the sliding testing. This phenomenon is a little different from those occurred for stainless steel [19], copper-base alloy [1], and other alloys [20,21]. It might be attributed to the remarkably different wear regimes of the diamond–Cu composite coating. Upon initiation of the sliding, the coating surface shows abundant copper which covers diamond particles. As sliding continues, many diamond particles are exposed and cannot be worn out. Consequently, the contact area between copper and Si_3N_4 ball decreases gradually, giving rise to less exposed active zone and less drop of OCP. When the friction is over, the OCP value rises abruptly in a quite short time and then gradually reaches the initial OCP of about −0.23 V, indicating recovery of the passive film.
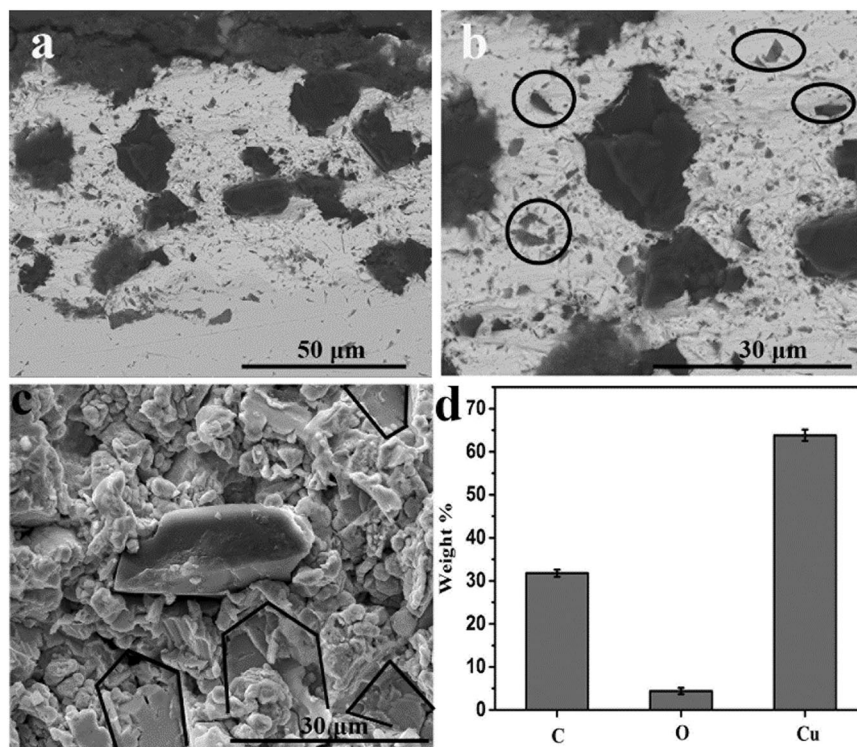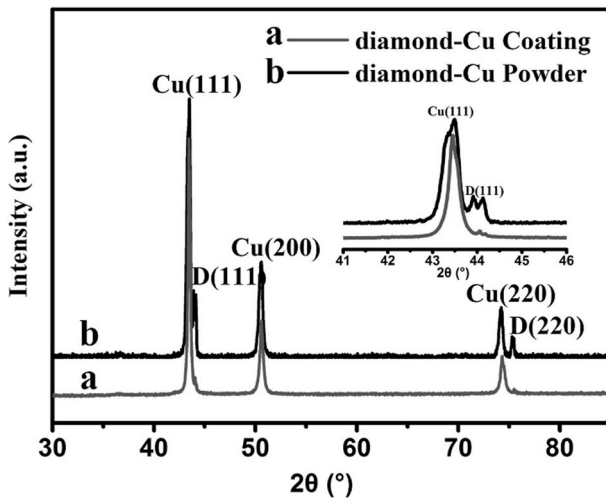
Figure 2. (a,b) SEM backscatter images showing cross-sectional morphology of the diamond–Cu composite coating ((b) is enlarged view of selected area in (a)), (c) SEM image showing surface morphology of the diamond–Cu composite coating, and (d) histogram of element contents of the diamond–Cu composite coating.

To further investigate the corrosion kinetics of the coatings during sliding, potentiodynamic polarisation spectrum is usually acquired [20]. For comparison purposes, the polarisation curves under corrosion-only and tribocorrosion conditions are shown in Figure 5 (b), and the values of the corrosion potential (E_{corr}) and the corrosion current density (I_{corr}) are provided in Table 1. The corrosion behaviour under corrosion-only condition could provide electrochemical information of materials without mechanical damage. It is clear that the passive region above 0 V of corrosion potential disappears for both the Cu coatings and the diamond–Cu composite coatings under the sliding conditions, indicating destruction of the passive film. Interestingly, under the sliding conditions, the diamond–Cu composite coating shows a smaller drop in E_{corr} drop and less increase in I_{corr} than those of the pure Cu coating. The measured corrosion current (I) can be considered as the sum of two partial current I_w and I_p, where I_w is the current acquired from the wear track area in which material is active, and I_p is the current acquired from the intact area in which material is passive. On the surface in passive state, I_p cannot exceed the current value measured at the


Figure 3. Schematic illustration showing the formation mechanisms of the diamond–Cu composite coating.

Figure 4. XRD curves of the diamond–Cu powder and the diamond–Cu coating.

Table 1. Corrosion potential (E_{corr}) and current density (I_{corr}) vlaues

Materials	Corrosion-only		Tribocorrision	
	E_{corr} (V)	I_{corr} (µA cm^{-2})	E_{corr} (V)	I_{corr} (µA cm^{-2})
316L	−0.3181	0.1098	−0.4323	0.4775
Cu	−0.2665	0.4337	−0.3334	5.869
Diamond–Cu	−0.295	0.4752	−0.2858	2.095

deformation (Figure 6(b)) and no obvious change in the surface morphology of the Si_3N_4 ball is seen (Figure 6(d)).

Figure 7 shows the evolution of friction coefficient (COF) for the 316L (∼0.49), the Cu coating (∼0.32), and the diamond–Cu coating (∼0.10). The COF displays similar features: after reaching the highest value, the COF begins to decrease until the wear reaches a relatively stable stage. However, the COF of the diamond–Cu coating goes abruptly to a value of around 0.45 at the beginning of the friction, which is very different from those of the 316L and the Cu coating. Generally, the rising stage of COF represents a run-in period and the decreasing stage arises from a rapid increase of the wear between ball and coating [22]. Although a strong wear dose exists between the diamond particles and the Si_3N_4 ball, it would not lead to such a boom in the COF. As it is well known that diamond has very low coefficient of friction [22], when hard diamond surface is sliding against a comparatively soft material, the soft material would wear out and fill the asperities of rough diamond surface and reduce its COF [23]. Thus, in this case, the fact that Si_3N_4 ball initially contacts with the coarse soft copper on the coating surface is presumably responsible for the slightly higher COF of the diamond–Cu coating during early stage sliding. As sliding continues, diamond particles get exposed and their intimate contact with the sliding ball is expected, which triggers the sharply dropped COF (Figure 7(a)). Moreover, the existence of diamond particles at the top surface of the coatings would protect the copper matrix against

same potential on the intact surface. By comparing the corrosion current values acquired under the corrosion-only and the tribocorrosion conditions, it can be found that the corrosion current is almost equal to I_w under the sliding condition. The result suggests that friction-induced dissolution plays a major role in regulating the tribocorrosion behaviours. Therefore, enhancing wear resistance should be one of the first considerations to improve the anti-tribocorrosion performances of the coatings in the marine environment.

To investigate the tribological behaviour of the diamond–Cu coatings in the marine environment, the worn surfaces of the tested coatings and Si_3N_4 balls were characterised by the SEM (Figure 6). No deep scars are seen from the surface of the diamond–Cu composite coating, while the spherical surface of the Si_3N_4 balls has been abraded to flat shape (Figure 6(a, c)). The retention of diamond particles after the abrasion indicates good interfacial bonding between diamond and copper matrix (Figure 6(a-2)). In contrast, however, the pure Cu coating suffers severe
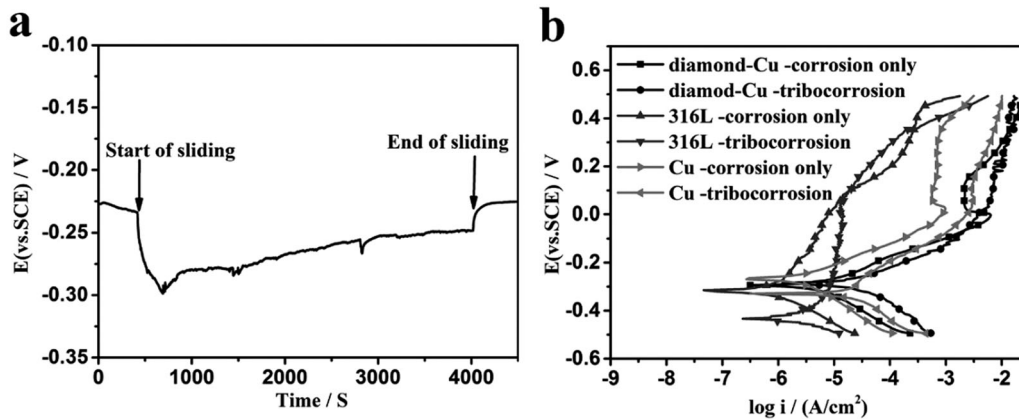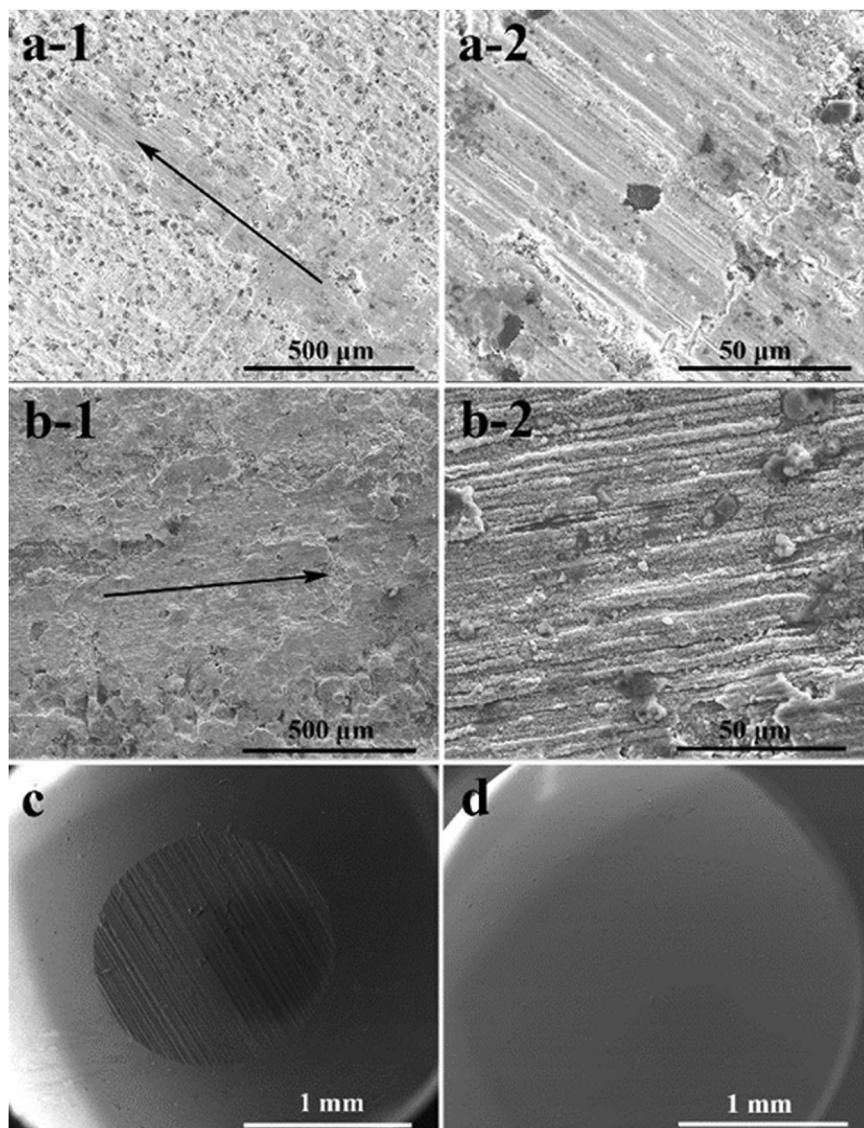

Figure 5. (a) Evolution of the OCP as a function of time and (b) polarisation curves measured under the corrosion-only and the tribocorrosion conditions.

Figure 6. SEM images of worn surfaces of the diamond–Cu coatings (a) and the pure Cu coatings (b) (-2 is enlarged view of selected area in -1), and topographical SEM images of the worn Si_3N_4 ball after being abraded by the diamond–Cu coating (c) and the pure Cu coating (d).

further wearing out greatly (Figure 7(b)). There is a giant disparity of wear volume between the diamond–Cu coating and the pure Cu coating. The enhanced wear/corrosion resistance of the diamond-containing coating indicates great potential of their applications in the marine environment.
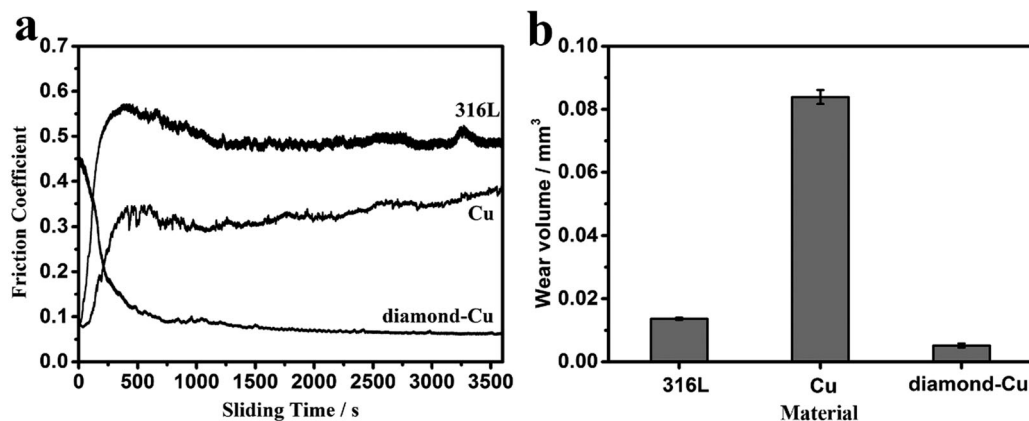
Figure 7. (a) Variations in friction coefficient with changes in sliding time and (b) wear volume loss of the samples after 60 min sliding testing in ASW.

Conclusions

Diamond–Cu composite coatings were successfully fabricated by CS the Cu-enwrapped diamond particles and the particles were prepared by the electroless plating. Diamond particles are well retained in the coatings and the diamond–Cu coatings show significantly enhanced anti-wear and anti-corrosion resistance as compared to the pure Cu coatings and 316L substrates. The electroless plating approach for diamond–Cu powder preparation and the cold spray route would open a new window for designing and constructing hard anti-corrosion coatings for marine applications in the areas involving high wear and tribocorrosion.

Disclosure statement

No potential conflict of interest was reported by the authors.

Funding

ORCID

Xiuyong Chen 🄳 http://orcid.org/0000-0001-5027-8631
Hua Li 🄳 http://orcid.org/0000-0002-8786-4295

References

[1] Kawazoe T, Ura A. Corrosive wear testing of metals in seawater. In: Totten GE, Wedeven LD, Dickey JR, Anderson M, editors. Bench testing of industrial fluid lubrication and wear properties used in machinery applications. Seattle: ASTM International; 2001. p. 296–305.

[2] Shan L, Zhang YR, Wang YX, et al. Corrosion and wear behaviors of PVD CrN and CrSiN coatings in seawater. Trans Nonferr Met Soc China. 2016;26:175–184.

[3] Lei X, Wang L, Shen B, et al. Microdrill with variations in thickness of diamond coating. Surf Eng 2016;32:165–171.

[4] Wasy A, Balakrishnan G, Lee S, et al. Thickness dependent properties of diamond-like carbon coatings by filtered cathodic vacuum arc deposition. Surf Eng 2015;31:85–89.

[5] Venkateswarlu K, Rajinikanth V, Naveen T, et al. Abrasive wear behavior of thermally sprayed diamond reinforced composite coating deposited with both oxyacetylene and HVOF techniques. Wear. 2009;266:995–1002.

[6] Tillmann W, Vogli E, Nebel J, et al. Influence on diamonds during the spraying of diamond-bronze abrasive coatings. J Therm Spray Technol. 2010;19:350–357.

[7] Leech PW, Li XS. Comparison of abrasive wear in diamond composites and WC-based coatings. Wear. 2011;271:1244–1251.

[8] Wang HR, Li WY, Ma L, et al. Corrosion behavior of cold sprayed titanium protective coating on 1Cr13 substrate in seawater. Surf Coat Technol. 2007;201:5203–5206.

[9] Huang CJ, Li WY. Strengthening mechanism and metal/ceramic bonding interface of cold sprayed TiNp/Al5356 deposits. Surf Eng. 2016;32:663–669.

[10] Koivuluoto H, Vuoristo P. Structure and corrosion properties of cold sprayed coatings: a review. Surf Eng. 2014;30:404–413.

[11] Li CJ, Suo XK, Yang GJ, et al. Influence of annealing on the microstructure and wear performance of diamond/NiCrAl composite coating deposited through cold spraying. In: Chandra T, Wanderka N, Reimers W, Ionescu M, editors. Thermec 2009, Pts 1-4. Zurich: Trans Tech Publications Ltd; 2010. p. 894–899.

[12] Na H, Bae G, Shin S, et al. Advanced deposition characteristics of kinetic sprayed bronze/diamond composite by tailoring feedstock properties. Compos Sci Technol. 2009;69:463–468.

[13] Li WY, Li CJ, Liao HL. Effect of annealing treatment on the microstructure and properties of cold-sprayed Cu coating. J Therm Spray Technol. 2006;15:206–211.

[14] Yao JH, Yang LJ, Li B, et al. Beneficial effects of laser irradiation on the deposition process of diamond/Ni60 composite coating with cold spray. Appl Surf Sci. 2015;330:300–308.

[15] Chen J, Wang J, Yan F, et al. Assessing the corrosion-wear behaviours of Hastelloy C276 alloy in seawater. Lubr Sci. 2016;28:67–80.

[16] Tekin KC, Malayoglu U. Assessing the tribocorrosion performance of three different nickel-based superalloys. Tribol Lett. 2010;37:563–572.

[17] Sun Y, Rana V. Tribocorrosion behaviour of AISI 304 stainless steel in 0.5 M NaCl solution. Mater Chem Phys. 2011;129:138–147.

[18] Diomidis N, Celis JP, Ponthiaux P, et al. Tribocorrosion of stainless steel in sulfuric acid: identification of corrosion-wear components and effect of contact area. Wear. 2010;269:93–103.

[19] Chen J, Yan FY. Corrosive wear performance of Monel K500 alloy in artificial seawater. Tribol Trans. 2013;56:848–856.

[20] Chen J, Zhang Q, Wang J, et al. Electrochemical effects on the corrosion-wear behaviors of NiCrMo-625 alloy in artificial seawater solution. Tribol Trans. 2016;59:292–299.

[21] Shan L, Wang Y, Li J, et al. Effect of N-2 flow rate on microstructure and mechanical properties of PVD CrNx coatings for tribological application in seawater. Surf Coat Technol. 2014;242:74–82.

[22] Konicek AR, Grierson DS, Gilbert PUPA, et al. Origin of ultralow friction and wear in ultrananocrystalline diamond. Phys Rev Lett. 2008;100:49.

[23] Jana A, Dandapat N, Das M, et al. Severe wear behaviour of alumina balls sliding against diamond ceramic coatings. Bull Mater Sci. 2016;39:573–586.